NONLINEAR AERODYNAMIC IDENTIFICATION AND STALL FLUTTER ANALYSIS

XIANG ZhengPing[1] , DAI YuTing[1]

[1]School of Aeronautic Science and Engineering，Beihang University , Beijing, China
zhengpingxiang@buaa.edu.cn

Keywords: *OpenFOAM*; Limit Cycle Oscillation; Unsteady aerodynamics; Stall flutter; Neural network;

Abstract: A solver has been developed within the *OpenFOAM* framework to compute large amplitude motion of a two-dimensional rigid airfoil. The aerodynamic force obtained with this code is successfully validated by experimental data. On the basis of this, the bifurcation point and the Limit Cycle Oscillations of the NACA0012 airfoil are simulated. Then ,using the nonlinear aerodynamic data calculated by CFD, a nonlinear aerodynamic identification method is developed based on neural network method. This method laid the foundation for the analysis of the limit cycle oscillation.

1 INTRODUCYION

Stall flutter is a nonlinear and self-excited aeroelastic phenomenon that can affect wind turbine blades, aircraft empennages, highly flexible wings, and non-airfoil structures[1]. Unlike linear bending-torsion flutter where at least two modes interact to generate hazardous oscillations of exponentially increasing amplitudes[2] and dynamic stall, which is a purely aerodynamic nonlinear phenomenon associated with large region of separated flows[3],stall flutter can involve a single mode by coupling aerodynamic nonlinearities with structural restoring forces to generate self-sustained Limit Cycle Oscillations (LCO)[4].

McCroskey [5] first defined two stall forms: deep stall and shallow stall. In 1960s, Ham and Young [6] defined the stall flutter of the wing or helicopter blades. In 1970s, Ericsson and Reding[7-9] made a lot of work on dynamic stall. They proposed a quasi-constant aerodynamic model about two-dimensional wing dynamic stall with trailing edge shedding vortices, and further analysis of the impact of the leading edge shedding vortices[10]. Since 1980, the simulation model about dynamic stall and stall flutter was developing continuously. Wernert [11] has made significant progress in predicting the dynamic stall of two-dimensional rigid body airfoils. On this basis , people began to study stall flutter gradually. In 2009, Dimitriadis and Li [12] made some experimental studies on the pitch and plunge degrees of freedom of the NACA0012 wing. In 2012, Sacha Yabili [4] simulated the dynamic stall and stall flutter of the binary wing under the low Reynolds number, and the calculated results were in good agreement with the experimental results made by Dimitriadis and Li.

The accuracy of experimental study and CFD calculation is higher, but the cost is high and time consuming. In addition, when the grid scale is large, CFD calculation is time-consuming and the computer hardware requirements are higher, increasing the cost of computing. In recent years, unsteady aerodynamic reduced order model based on CFD technology have been developed rapidly [13-15] .The technique achieves the similar precision to the CFD through the lower order model, but the computational efficiency is improved by one or two orders of magnitude. Unsteady aerodynamic reduction model based on CFD is mainly divided into proper orthogonal decomposition (POD)[16], based on the system identification[17]and based on the harmonic balance (HB) technology[18] .

In this paper, *OpenFOAM* open source code is used to simulate the dynamic stall and stall flutter of NACA0012 wing and analyze the mechanism of occurring stall flutter. Then, the CFD method is used to calculate the training signal, and the BP neural network model with output feedback is used to establish the dynamic time-domain nonlinear aerodynamic model under low-speed large attack angle. The identification results and CFD result are compared to verify the performance of the identify system.

2 COMPUTATIONAL METHODOLOGY

The accurate simulation of the complete stall flutter mechanism is very challenging and requires an efficient of high amplitude motions, as well as an accurate prediction of the flow separation and reattachment process[4]. The *OpenFOAM* open source slover has been applied to this stall flutter investigation.

2.1 Unsteady flow field solving method

In the inertial coordinate system, the Navier-Stokes equation of unsteady integral form can express as

$$\frac{\partial}{\partial t}\int_{\Omega(t)} \vec{U} d\Omega + \int_{S(t)} \vec{F} \bullet d\vec{S} = \frac{1}{Re}\int_{S(t)} \vec{F}_V \bullet d\vec{S} \tag{1}$$

Where $\vec{U}$ represents the flux that the mass, energy, and momentum of the unit volume. $\vec{F}$ and $\vec{F}_V$ are respectively represented no viscous flow vectors and viscous flow vectors. $\Omega(t)$ is motion control volume, $S(t)$ is surface area of motion control volume.

Finite-volume method for space-discrete, second-order upwind scheme, time marching is two order implicit scheme, PIMPLE algorithm were applied. Turbulence model is *k-w* SST turbulence model, which can handle flow separation well [19].

2.2 Grid and boundary conditions

Using the *blockMeshDict* and *snappyHexMeshDic* tools in *OpenFOAM* to divide the structure grid. The grid is adaptable and can withstand the large deformation. The grid is shown in Figure 1. Figure 1(a) is entire domain mesh and Figure 1(b) is mesh of near airfoil. the distance from inlet to leading edge of wing is 5 times chord, the distance from the outlet to trailing edge of wing is above 12 times chord . Slip boundary condition is applied to the upper and lower surfaces, The velocity inlet is the flow velocity, the velocity outlet is the inlet and

outlet boundary, and the boundary condition of the wing surface is *movingwallvelocity*. Pressure boundary conditions are *zeroGradient*.

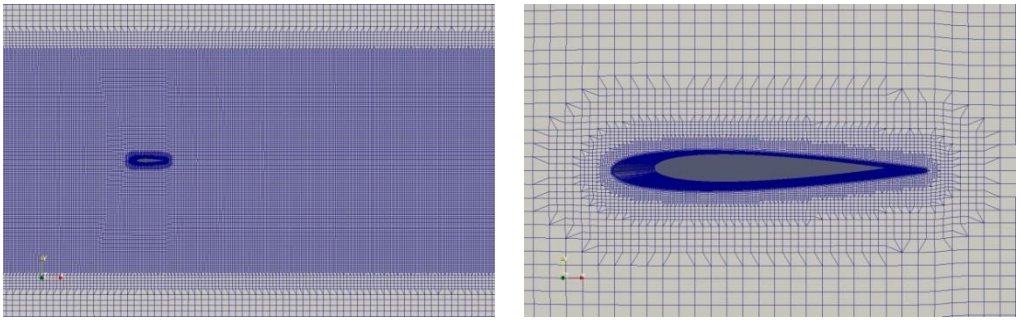

(a): Entire domain mesh (b): Mesh near airfoil

Fig1: Geometry of the computational domain and mesh used for simulations

2.3 Structural model and Coupling algorithm

When the structure and aerodynamic coupling, the equation of coupling can be expressed as

$$M\ddot{q}(t)+C\dot{q}(t)+Kq(t)=F(t) \tag{2}$$

Where M,C,K are the structural mass, damping and stiffness matrices, respectively, and F is the vector of the external forces. Matrices M,C,K are obtained from the experimental wind-off data[1].At the n^{th} iteration of the aeroelastic with *OpenFOAM* , the equation of motion are expressed as

$$\begin{bmatrix} m & S_\alpha \\ S_\alpha & I_\alpha \end{bmatrix}\begin{pmatrix} \ddot{h}_n \\ \ddot{\alpha}_n \end{pmatrix}+\begin{bmatrix} c_h & 0 \\ 0 & c_\alpha \end{bmatrix}\begin{pmatrix} \dot{h}_n \\ \dot{\alpha}_n \end{pmatrix}+\begin{bmatrix} k_h & 0 \\ 0 & k_\alpha \end{bmatrix}\begin{pmatrix} h_n \\ \alpha_n \end{pmatrix}=\frac{1}{2}\rho cv\begin{pmatrix} C_{Ln} \\ cC_{Mn} \end{pmatrix} \tag{3}$$

Where *h* is the plunge displacement and α is the pitch angle. The external forces expressed as lift and pitching moment coefficients on the right hand side of this equation are obtained from the CFD solver. Numerous algorithms, such as *Runge-Kutta* methods[20] can be used to solve equation (3).

3 DYNAMIC STALL AND STALL FLUTTER SIMULATION

3.1 Dynamic stall

It is necessary to verify the correctness of the computational method before simulating stall flutter. The verification is divided into two parts. First, the accuracy of the solver is verified. The first test case was used to validate the forced motion capabilities of *OpenFOAM* for a NACA0012 airfoil pitching with a mean angle of 0^o ,a 5^o amplitude and a reduced frequency equal to 0.2. The low amplitude of these oscillations was chosen to demonstrate that the solver correctly predicts the flow around an oscillating airfoil without the strong boundary layer separation that occurs at higher amplitudes. The results obtained are compared on Figure2(a) with numerical solutions obtained with the *OVERFLOW* solver, which has already been validated for similar applications[21],It can be seen that a very good agreement is obtain for the lift coefficient.

The second test case evaluated a NACA 0012 airfoil pitching with a mean angle of 10^0

an 15^0 amplitude of oscillation at a reduced frequency equal to 0.2. Figure2(b) , (c), (d) compares the numerical solution with experimental data obtained by Lee[22]. It can be seen that the high degree of nonlinearity generated by a complex flow separation and reattachment process is difficult to capture with accuracy. Nonetheless it is fair to say that the trends of the aerodynamic coefficients are well simulated by *OpenFOAM*.

The differences in the correlation between the numerical and experimental data may be due to various sources. In particular, the free stream turbulence intensity at the time of the experiment is not known, and it may significantly influence the numerical results[23].

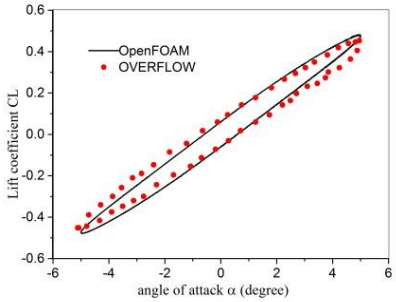

(a) CL VS α

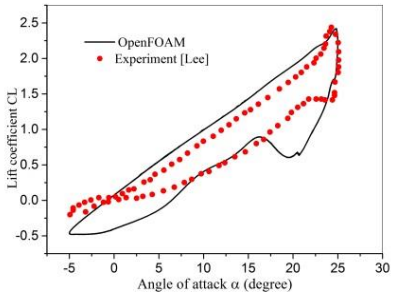

(b) CL VS α

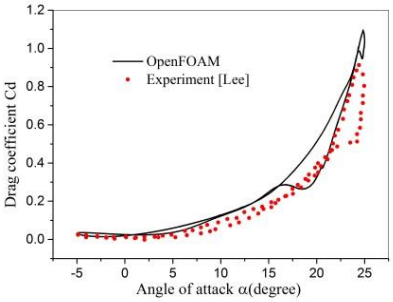

(c) Cd VS α

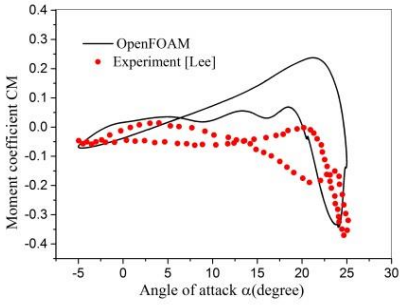

(d) Cm VS α

Fig2:Aerodynamic coefficient for a NACA0012 airfoil undergoing pitch motion

3.2 Stall flutter

On the basis of dynamic stall, the stall flutter is simulated. The structural parameters are shown in Table 1. Since the stall flutter is caused by the coupling of the pitch mode and the aerodynamic force, the stiffness in plunge is large and the stiffness in pitch is small.

Simulation parameter	Value	Simulation parameter	value
Wing span	1m	Wing chord	1m
Pitch axis position	0.4m	Airspeed	0-25m/s
Weight of wing assembly	51kg	Moment of inertia around pitch axis	3.2kg.m^2
Stiffness in plunge	60N/mm	Stiffness in Pitch	105N.m/rad

Table1：Important Structural parameters

The response of wing under 0-25m/s is computed respectively. The result is shown in

Figure 3. It is found that when the airspeed is below 12m/s, no matter how large the initial attack angle is, the oscillations will converge. The bifurcation velocity is about 12.5m/s, and the amplitude of the limit cycle oscillation increases with the increase of velocity. The response at a speed of 12 m/s is shown in Fig4. When the speed reaches 12.5m/s, the limit cycle oscillation occurs as shown in figure5.Figure6 shows the response at v=16m/s.

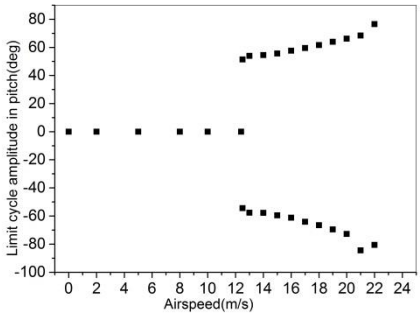

Fig3:Bifurcation and Limit cycle amplitude

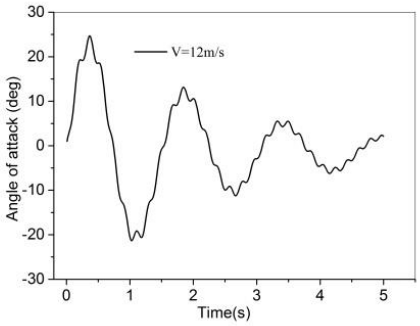

Fig4: Pitch variations at v=12m/s

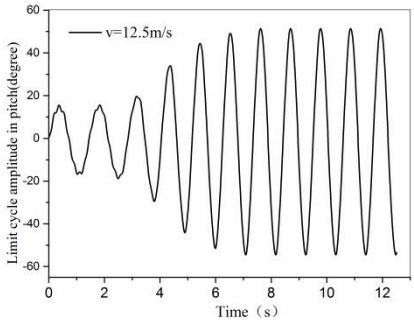

Fig5: Pitch variations at v=12.5m/s

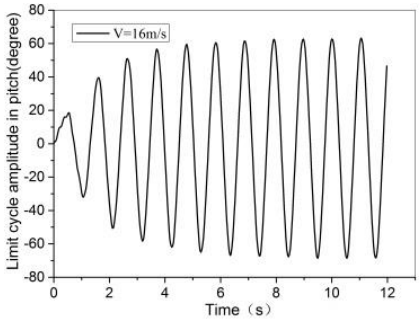

Fig6: Pitch variations at v=16m/s

In order to describe the limit cycle oscillations in more detail, the responses of lift coefficient, drag coefficient and moment coefficient are shown in figure 7,8,9 when the airspeed is 16m/s. Figure7(a) is the response of lift coefficient with time and Figure7(b) is the response of lift coefficient with angle in one cycle. We can see that there is an obvious stall near the maximum amplitude. Figure8(a),(b) are drag coefficient responses with time and angle. Figure9(a),(b) are moment coefficient responses with time and angle.

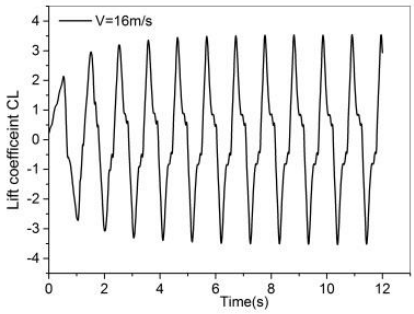

(a) CL vs Time

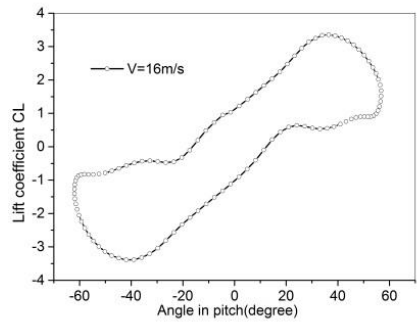

(b) CL vs Angle

Fig7:Response of lift coefficient

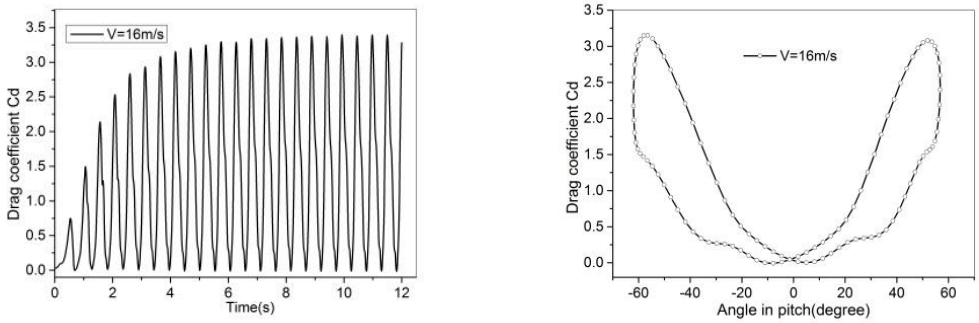

(a) Cd vs Time (b) Cd vs Angle

Fig8: Response of drag coefficient

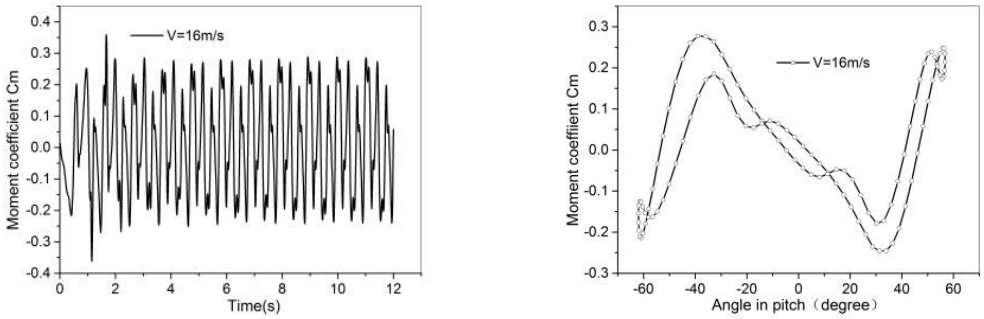

(a) Cm vs Time (b) Cm vs Angle

Fig9: Response of moment coefficient

In order to explain the process of flow separation and reattachment and vortex shedding in the limit cycle oscillations more clearly, the pressure contours are shown as Figure10 in half a cycle at v=16m/s. In order to sustain the oscillation the fluid has to inject energy to the structure during each cycle. The mechanism for this injection of energy is the generation and shedding of a leading edge vortex.

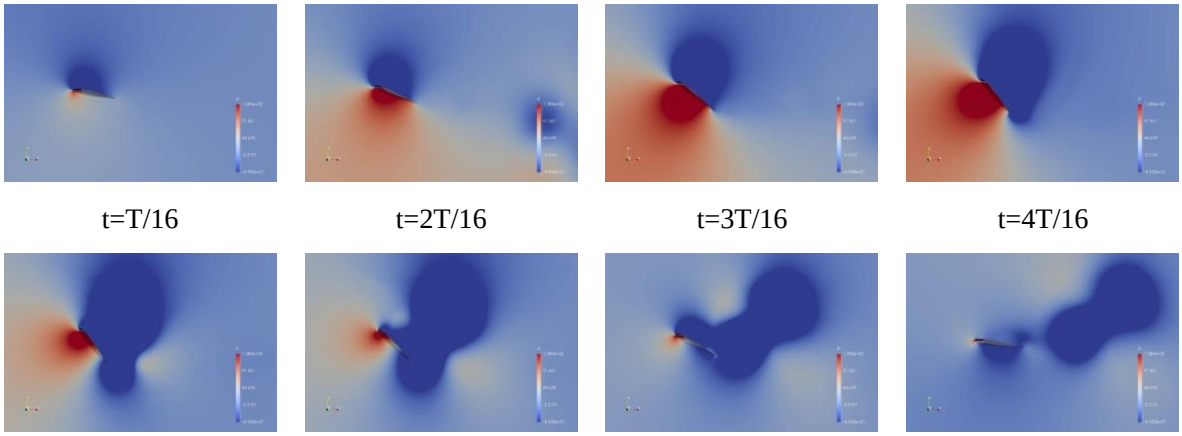

t=T/16 t=2T/16 t=3T/16 t=4T/16

t=5T/16 t=6T/16 t=7T/16 t=8T/16

Fig10 Pressure nephograms in half a cycle at v=16m/s

4 UNSTEADY AERODYNAMIC IDENTIFICATION

Because of the complexity of the nonlinear flow field, the traditional model requires high experience and it is difficult to give a suitable display expression. The Neural Network (NN)

model has the advantage of not giving the display mathematical expression between the input / output identification system[24].

4.1 Back-Propagation (BP) Network

The basic idea of the BP neural network is that the learning process consists of two processes, the forward propagation of the signal and the back propagation of error. Taking the single hidden layer BP network as an example, the network structure diagram is shown in figure 11.

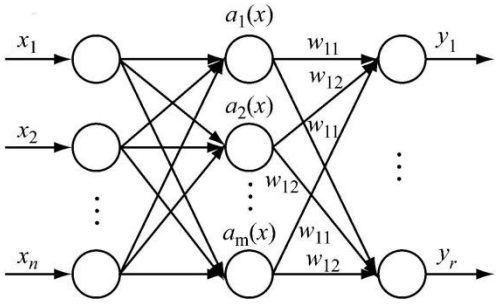

Fig11: BP network with single hidden layer

In the three layer feedforward network, $X = (x_1, x_2, ..., x_i, ..., x_n)^T$ is input vector. The hidden layer is $a_i(x)\ \ i = 1, 2...m$. $O = (o_1, o_2, ..., o_i, ..., o_m)^T$ is output vector of the hidden layer, The output vector of the output layer is $Y = (y_1, y_2, ..., y_k, ..., y_r)^T$. The expected output vector is $D = (d_1, d_2, ..., d_k, ..., d_r)^T$. The weight matrix between the input layer and the hidden layer is represented by V, $V = (v_1, v_2, ..., v_j, ..., v_m)$. Where the column vector v_j is the weight vector of the j[th] neuron of the hidden layer. The weight matrix between the hidden layer and the output layer is represented by $W, W = (w_1, w_2, ..., w_k, ..., w_r)$, Where the column vector w_k is the weight vector of the K[th] neuron of the output layer. The relationship between them can be expressed as

$$y_k = f(net_k) \qquad k = 1,2,...r \qquad (4.1)$$

$$net_k = \sum_{j=0}^{m} w_{ik} o_j \qquad k = 1,2,...r \qquad (4.2)$$

$$o_j = f(net_j) \qquad j = 1,2,...m \qquad (4.3)$$

$$net_j = \sum_{i=0}^{n} v_{ij} x_j \qquad j = 1,2,...m \qquad (4.4)$$

The error function is

$$e = \frac{1}{2}\sum_{i=1}^{r}(d_i - y_i)^2 \qquad (4.5).$$

In forward propagation, the input samples are imported from the input layer, and then transmitted to the output layer through hidden layers. If the actual output does not correspond to the desired output, then the error is propagated backwards. The error signal is the basis of correcting the weight of each unit. Weights are constantly adjusted, and this process is the network learning and training process. This process continues until the output error reduced to the expected value.

4.2 BP network with feedback

Here, the forced vibration of pitching motion is taken as an example .When standard BP network is used to identify time-domain aerodynamic forces, displacement u （$u=\{\alpha\}$， α is pitch angle）is input, Aerodynamic coefficient y（$y=\{C_L,C_m\}$， C_L,C_m is lift coefficient and drag coefficient）is output. Consider the unsteady hysteresis effect of the flow field, the m order delay of u is introduced, input vector $x_k=[u_k,u_{k-1},...u_{k-m}]^T$. The standard BP network is essentially a quasi-regular model, The m-order delay network has only m discrete steps, and the current output is affected only by the current and m-order inputs. This model only approximates the accurate unsteady model when m is large enough. However, when them is too large, the more time required for training signals, the longer the CFD time required to obtain the signal. To solve these problems, a BP model with feedback is proposed, in which the output and input of the network are used as input. The BP network with feedback can be expressed as $\{y_k\}^T=f(u_k,u_{k-1},u_{k-2},...,u_{k-m},y_{k-1},y_{k-2},...,y_{k-n})$. The schematic diagram of the BP network with output feedback is shown in Figure 12. After introducing dynamic delay, The K^{th} order input u_k can affect any subsequent output $y_k^{'}$. In addition, for a trained network, the effect of u_k on $y_k^{'}$ will decay as $k^{'}-k$ increases. Therefore, the BP model with output feedback is an unsteady aerodynamic model.

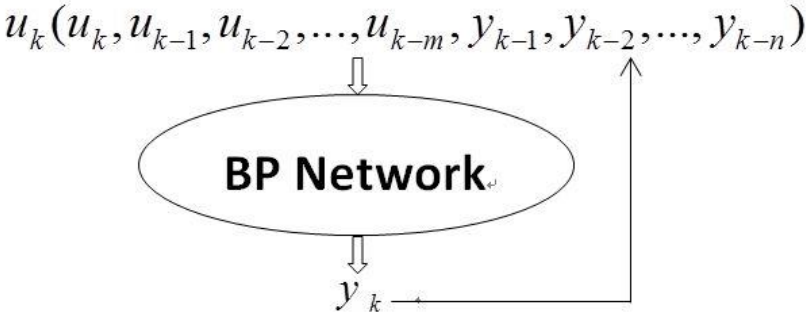

Fig12: BP model with feedback

4.3 Test case

When training the network, the training data should include as much information as possible. In this case, the input angle α varies with time to include the desired frequency and amplitude. When wing vibrates with large amplitude, the vibration frequency is generally less than 5Hz. Therefore, the training signal should include these frequencies. Training signal can be expressed as

$$\alpha=3sin(2\pi t)+5sin(4\pi t)+10sin(8\pi t)+16sin(16\pi t) \tag{5}$$

The response of input angle α over time and the corresponding lift coefficient computed by CFD are shown in Figure13 and Figure 14. It can be seen that their trends are similar. Figure15 shows the comparative results between identification results and CFD results. Ident is BP network without feedback and Ident1is BP network with feedback. In order to see the difference more clearly, the partial magnification is shown in Figure16. It's found that the result of Ident1 is in better agreement with the CFD result. Figure17 shows the error from BP network without feedback and figure18 shows the error from BP network with feedback.

Obviously, BP network with feedback is more accurate. The delay orders and average error of both models are listed in Table 2.

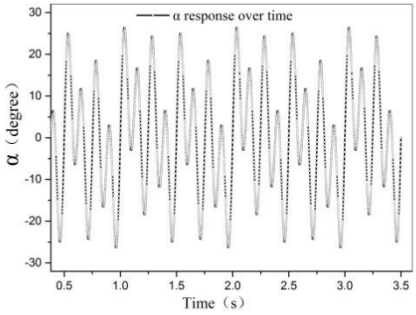

Fig13:Input angle response over time

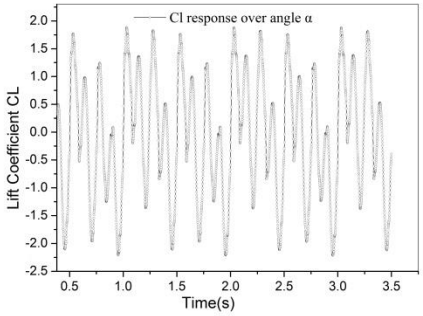

Fig14:Lift coefficient response over α

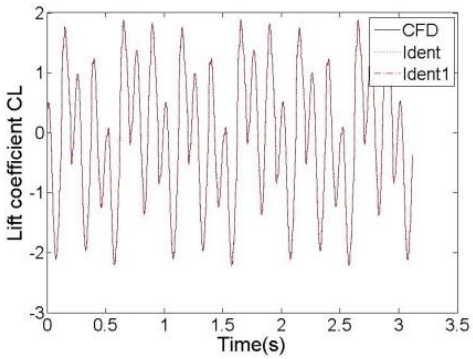

Fig15: Comparison between ident and CFD

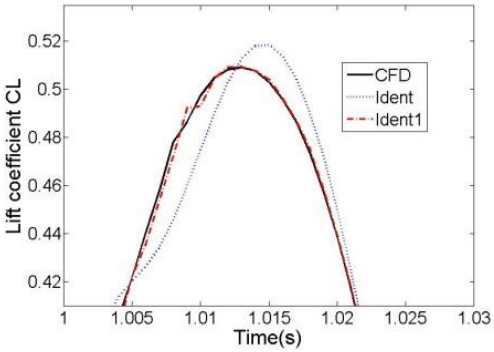

Fig16: Partial magnification region

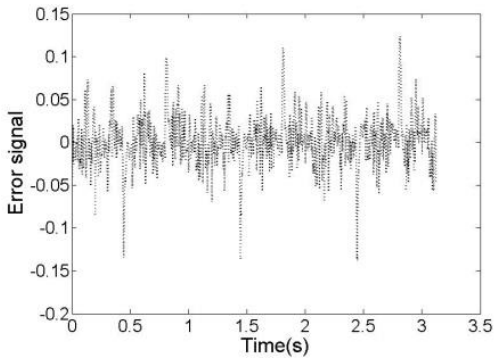

Fig17: Error from Ident

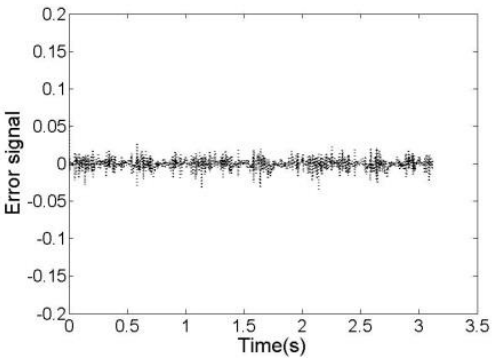

Fig18: Error from Ident1

Test case	Delay orders	average error	Training time
BP network without feedback	m=20	0.001	about 1min
BP network with feedback	m=3,n=3	0.00001	about 0.5 min

Table2：Comparison of the two models

By comparison, we can see that the BP neural network with output feedback can be used for the identification of nonlinear unsteady aerodynamic forces after proper training, which can greatly improve the simulation efficiency of complex dynamics in nonlinear flow field. The calculations main focus on the CFD calculation to obtain the training signal, which lasts about a few hours, but identification typically take only a few seconds.

5 CONCLUSION

1. A solver has been developed within the *OpenFOAM* framework to compute large amplitude motion of two-dimensional rigid airfoil. The results were correlated with experimental data.
2. The stall flutter of NACA0012 wing is numerically simulated. The bifurcation point velocity and the amplitude of the limit cycle oscillations at different speeds are obtained. The vibration process of the limit cycle oscillations is analyzed.
3. A BP neural network model with output feedback is developed. The model can identify the nonlinear unsteady aerodynamics at high attack angle, and the prediction accuracy is higher than the standard BP network. This method has laid a foundation for the analysis of limit cycle flutter in nonlinear flow field.

REFERENCES：

[1] Dimitriadis, G. and Li, J., “Bifurcation Behavior of Airfoil Undergoing Stall Flutter Oscillations in Low-Speed Wind Tunnel," AIAA Journal, Vol. 47, No. 11, 2009, pp. 2577-2596.

[2] Bisplingho, R., Ashley, H., and Halfman, R., Aeroelasticity, Addison-Wesley Publishing Company, Inc, 1955.

[3] Ekaterinaris, J. and Platzer, M., “Computational Prediction of the Airfoil Dynamic Stall," Progress in Aerospace Sciences.Vol. 33, No. 11-12, 1997, pp. 759-864.

[4] Sacha Yabili, Marilyn J. Smithy. Unsteady Navier-Stokes Simulation of Low-Reynolds Stall Flutter.AIAA,2012-37.

[5] McCroskey, W. J., “The Phenomenon of Dynamic Stall,” NASA TM 81264, 1981.

[6] Ham, N. D., and Young, M. I., “Torsional Oscillation of Helicopter Blades Due to Stall,” Journal of Aircraft, Vol. 3, No. 3, 1966, pp. 218–224.

[7] Ericsson, L. E., and Reding, J. P., “Unsteady Airfoil Stall,” NASA CR 66787, 1969.

[8] Ericsson, L. E., and Reding, J. P., “Analytic Prediction of Dynamic Stall Characteristics,” AIAA Paper 72-682, June 1972.

[9] [9] Ericsson, L. E., and Reding, J. P., “Stall-Flutter Analysis,” Journal of Aircraft, Vol. 10, No. 1, 1973, pp. 5–13.

[10] Ericsson, L.E., and Reding, J.P., “Dynamic Stall at High Frequency and Large Amplitude,” Journal of Aircraft, Vol. 17, No. 3, 1980, pp. 136–142.

[11] Wernert, P., Geissler, W., Raffel, M., and Kompenhans, J., “Experimental and Numerical Investigations of Dynamic Stall on a Pitching Airfoil,” AIAA Journal, Vol. 34, No. 5, 1996, pp. 982–989.

[12] Dimitriadis, G. and Li, J., Bifurcation Behavior of Airfoil Undergoing Stall Flutter Oscillations in Low-Speed Wind Tunnel, AIAA Journal, Vol. 47, No. 11, 2009, pp. 2577-2596.

[13] Dowell E H,Hall K C.Modeling of fluid-structure interaction[J],Annual Review of Fluid Mechanics.2001,33:445-490.

[14] Lu cai D J,Beran P S,Silva W A.Reduced-order modeling:new approaches for computations physics[J].Progress in Aerospace Science,2004, 40(1):51-117.

[15] Zh ang Weiwei , Ye Zh engyin .On uns teady aerodynamic modeling b ased on CFD technique and it s applicat ions on aeroel as tic analysis[J] .*Advances in Mechanics* ,

2008 , 38(1):77-86.
[16] Thomas JP, Dowell E H,Hall K C.Three-dimensional transonic aeroelasticity using proper orthogonal decomposition-based reduce-order models. *Journal of Aircraft*, 2003, 40(3): 544~551.
[17] Cowan TJ,Andrew SAJ,Gupta KK,Accelerating computational fluid dynamics based aeroelastic predictions using system identification, *Journal of Aircraft*, 2001, 38(1): 81~87.
[18] Thomas J,Hall KP,Dowell EH,A harmonic balance approach for modeling nonlinear aeroelastic behavior of wings in transonic viscous flow.AIAA paper 2003-1924,2003.
[19] Menter, F., 'Two-Equation Eddy-Viscosity Turbulence Models for Engineering Applications," AIAA Journal, Vol. 32, No. 8, August 1994, pp. 1598-1605.
[20] Forsythe, G. E., Malcolm, M. A., and Moler, C. B., Computer Methods for Mathematical Computations, Prentice-Hall,1977.
[21] Liggett, N. and Smith, M., Temporal Convergence Criteria for Time-Accurate Viscous Simulations of Separated Flows,"Under revision for the Journal of Computers and Fluids, 2011.
[22] Lee, T. and Gerontakos, P., Investigation of Flow Over an Oscillating Airfoil," Journal of Fluid Mechanics, Vol. 512,2004, pp. 313-341.
[23] Wang, S., Ma, L., Ingham, D. B., Pourkashanian, M., and Tao, Z., \Numerical Investigations on Dynamic Stall of Low Reynolds Number Flow Around Oscillating Airfoils," Computers and Fluids, Vol. 39, No. 9, 2010, pp. 1529-1541.
[24] Wang, S., Ma, L., Ingham, D. B., Pourkashanian, M., and Tao, Z., Numerical Investigations on Dynamic Stall of Low Reynolds Number Flow Around Oscillating Airfoils," Computers and Fluids, Vol. 39, No. 9, 2010, pp. 1529-1541.

COPYRIGHT STATEMENT